Heliyon 10 (2024) e29275

Contents lists available at ScienceDirect

Heliyon

journal homepage: www.cell.com/heliyon

Research article

Clinical significance of immune-related antigen CD58 in gliomas and analysis of its potential core related gene clusters

Zhi Tian [a,1], Wei Jia [b,1], Zhao Wang [a], Hui Mao [a], Jingjing Zhang [a], Qiongya Shi [b], Xing Li [b], Shaoyu Song [a], Jiao Zhang [a], Yingjie Zhu [a], Bo Yang [c], Chunhai Huang [a,**], Jun Huang [d,*]

[a] Department of Neurosurgery, First Affiliated Hospital, Jishou University, Jishou, Hunan, 416000 PR China
[b] Medical College of Jishou University, Jishou, Hunan, 416000 PR China
[c] Department of Pathology, First Affiliated Hospital, Jishou University, Jishou, Hunan, 416000 PR China
[d] Department of Neurosurgery, Xiangya Hospital, Central South University, Changsha, Hunan 410008 PR China

ARTICLE INFO

Keywords:
CD58
Glioma
Prognosis
Mechanism
Immune
Antigen

ABSTRACT

Background: The clinical significance of immune-related antigen *CD58* in gliomas remains uncertain. The aim of this study was to examine the clinical importance and possible core related genes of CD58 in gliomas.
Methods: Pan-cancer analysis was to observe the association between *CD58* and different tumors, glioma RNA sequencing data and clinical sample analyses were used to observe the relationship between *CD58* and glioma, shRNA interference models were to observe the impact of *CD58* on glioma cell function, and four glioma datasets and two online analysis platforms were used to explore the core related genes affecting the correlation between *CD58* and glioma.
Results: High *CD58* expression was associated with worse prognosis in various tumors and higher malignancy in glioma. Down regulation of CD58 expression was linked to decreased proliferation, increased apoptosis, and reduced metastasis in glioma cells. The pathways involved in *CD58*-related effects were enriched for immune cell adhesion and immune factor activation, and the core genes were *CASP1, CCL2, IL18, MYD88, PTPRC,* and *TLR2*. The signature of *CD58* and its core-related genes showed superior predictive power for glioma prognosis.
Conclusion: High *CD58* expression is correlated with more malignant glioma types, and also an independent risk factor for mortality in glioma. *CD58* and its core-related genes may serve as novel biomarkers for diagnosing and treating glioma.

1. Introduction

Glioma, considered the most common primary intracranial malignancy, poses a significant threat to human health. In China, the

* Corresponding author. Department of Neurosurgery, Xiangya Hospital, Central South University, 87 Xiangya Road, Changsha City, Hunan Province, 410008, PR China.
** Corresponding author. Department of Neurosurgery, First Affiliated Hospital, Jishou University, the intersection of Jianxin Road and Qianzhou Shiji Avenue, Jishou City, Hunan Province, 416000, PR China.
E-mail addresses: huangchunhai2001@163.com (C. Huang), xxyyhj@csu.edu.com (J. Huang).
[1] Zhi Tian and Wei Jia contribute equally to this work.

https://doi.org/10.1016/j.heliyon.2024.e29275
Received 23 March 2024; Accepted 3 April 2024
Available online 9 April 2024

annual incidence rate of glioma is as high as 6.4/100,000 and continues to rise [1]. Due to its short disease course, aggressive invasion, and restricted by the blood-brain barrier, current treatment methods such as surgery, radiotherapy, and chemotherapy often fail to achieve satisfactory results, especially for patients with glioblastoma (GBM) [2,3]. Therefore, it is necessary and urgent to research new treatment methods and strategies for glioma.

Notablely, studies have suggested possible communication between the central nervous system and the immune system. Increased expression of immune components recruits immune cells across the blood–brain barrier [4–6]. Moreover, studies have proved that the development, treatment, and prognosis of gliomas are affected by immune function and levels of immune-related molecules in patients [7]. Clinical trials have shown that targeting gliomas with immunotherapy is associated with clinical benefits, exhibiting an important role of immune system in glioma progression [8–14].

CD58, or lymphocyte functional antigen-3 (*LFA-3*), is located on the surface of immunological and immune-related cells and is essential for normal immune function [15,16]. Several studies have revealed that *CD58* may affect tumor development through immune-related processes, such as the stimulation and multiplication of Natural killer (NK) cells, control of antiviral responses, regulation of inflammatory responses, and activation of immune evasion [17–20].

CD58 has been found to exhibit similar effects in gliomas. The expression of lymphocyte adhesion molecules, including *CD58,* has been observed in gliomas [21–23]. Exogenous SLFA3/T11TS, a *CD58*-like glycoprotein isolated from sheep erythrocytes, has been shown to induce regression of gliomas in rats and apoptosis of the neural neoplastic cells [24,25]. Data from The Encyclopedia of DNA Elements (ENCODE) suggest that *CD58* may function as one of the NF-κB binding sites involved in glioma progression [26]. Wu et al. also found that the $CD2^{-}CD58$ axis is involved in the progression of low-grade gliomas with the cancer genome atlas program (TCGA) database [27]. However, large-scale population analysis on the correlation between *CD58* and the prognosis of glioma, as well as reports on the gene clusters involved in *CD58* function in gliomas, are currently lacking.

The purpose of this study is to confirm the clinical significance of *CD58* in gliomas and explore potential gene clusters related to *CD58* activity. To achieve this goal, the researchers conducted analyses from three aspects: glioma-related biological databases (including European, American and Chinese populations), glioma clinical samples, and cell models. The research process is exhibited in Fig. 1.

2. Materials and methods

2.1. Pan-cancer analysis

We performed pan-cancer analysis of *CD58* expression using Sangerbox online platform (http://sangerbox.com/) [28]. We used the gene expression differential, gene expression prognostic, tumor stemness, and immune infiltration analyses in the "Single gene pan-cancer analysis" module of Sangerbox. The data for this pan-cancer analysis were obtained from the University of California, Santa Cruz (UCSC) database (N = 19131, G = 60499) and standardized uniformly.

2.2. Downloading and cleaning of glioma-related datasets

Four glioma-related datasets were utilized in this study: The Chinese Glioma Genome Atlas (CGGA), TCGA, GSE16011 and Rembrandt. TCGA, CGGA, and Rembrandt datasets were gained from the CGGA online platform (http://www.cgga.org.cn/), a user-friendly web application that explores brain tumor datasets from Chinese cohorts [29,30]. The CGGA platform's own RNA-sequencing data were Fragments Per Kilobase per Million (FPKM) values, and log 2 fold changes in the FPKM value served to represent the

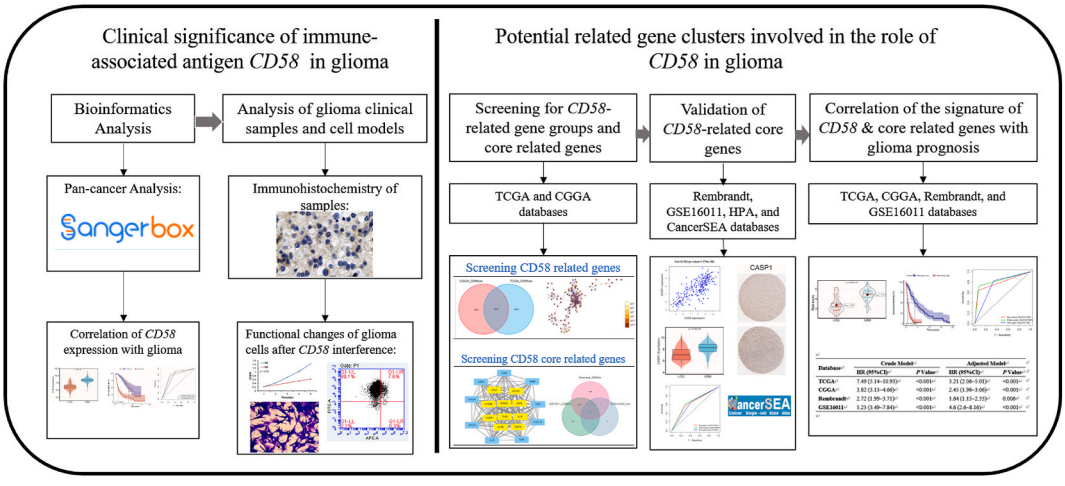

Fig. 1. Workflow. Clinical significance of *CD58* in glioma was investigated by glioma related databases, clinical samples, and cell models. Four glioma datasets and two online analysis platforms were used to explore the core related genes affecting the correlation between *CD58* and glioma.

expression level. In total, 1018 samples were selected from the CGGA dataset. The CCGA platform also provides TCGA and Rembrandt Gliom datasets for download. The TCGA glioma dataset consists of 720 samples with RNA-seq expression data (TPM) and clinical details. The Rembrandt glioma dataset consists of 450 samples along with microarray expression data [robust multichip average (RMA) algorithm standardization] and clinical information. We obtained the GSE16011 dataset from the Gene Expression Omnibus (GEO) database (https://www.ncbi.nlm.nih.gov/geo/), containing 276 glioma samples [31]. The microarray data was standardized using the RMA algorithm and accompanied by corresponding clinical information.

The data were subsequently cleaned. Samples with missing gene expression data or clinical information were excluded. The exclusion parameters for each database were as follows: TCGA: non-glioma (33), age missing (60), survival missing (6); CGGA: age missing (1), tissue type missing (5), censor missing (38), survival missing (9), radiotherapy status missing (34), chemotherapy status missing (11), IDH mutation status missing (47), 1p19 codeletion status missing (66), MGMTp methylation status missing (121); Rembrandt: age missing (80), sex missing (77), grade missing (38), censor missing (39), survival missing (28); GSE16011: Censor missing (120), survival missing (3). After excluding samples with missing variables, TCGA, CGGA, Rembrandt, and GSE16011 had 603, 686, 213, and 153 samples, respectively, for subsequent analyses.

2.3. Data analysis methods used in glioma datasets

The cut-off values used for the different gene expression or risk score groups were the median values of the gene expression values or risk scores (calculated as described later). Comparisons of baseline data across subgroups, and those of gene expression or risk scores across glioma subtypes were performed using the 'stats' package of R software version v4.3.0 (The R Foundation, http://www.R-project.org). The subsequent versions of R were the same. We utilized the Kaplan–Meier (KM) method and the log-rank test from the R packages 'survival' and 'survminer' to estimate survival curves. Additionally, we conducted time-dependent Receiver Operating Characteristic (ROC) curve analysis using the R package 'timeROC' to demonstrate the effectiveness of diverse factors in predicting mortality in glioma patients.

Cox proportional hazards models were developed using the 'Survival' package of R. *CD58*-associated Cox regression models were utilized to analyze the relationship between *CD58* expression groups and glioma mortality. Risk scores were computed using multivariate Cox regression models that were adjusted for the expression values of CD58 and other core-related genes (see later). Calculation formulas for each database were as follows:

TCGA: Risk Score = *CD58**0.745+*CASP1**0.625 +*CCL2**0.267+*IL18**0.448

+*MYD88**1.219+*PTPRC**0.360+*TLR2**0.415;

CGGA: Risk Score = *CD58**0.601+*CASP1**0.399+*CCL2**0.180+*IL18**0.254

+*MYD88**0.552+*PTPRC**0.281+*TLR2**0.387;

Rembrandt: Risk Score = *CD58**0.670+*CASP1**0.510+*CCL2**0.210

+*IL18**0.249+*MYD88**0.648+*PTPRC**0.481+*TLR2**0.385;

GSE16011: Risk Score = *CD58**0.502+*CASP1**0.307+*CCL2**0.174

+*IL18**0.195+*MYD88**0.585+*PTPRC**0.201+*TLR2**0.248.

Cox regression models adjusted for separate variables were also used to analyze the correlation between risk score categories and the mortality of glioma.

Subgroup analysis was conducted to examine the association between *CD58* expression and mortality of glioma subgroups divided according to age, sex, histology, and grade. The adjusted Cox regression model employed interaction testing to compare hazard ratios (HRs) across the examined subgroups. The R package 'survminer' was to draw the forest map for subgroup analysis.

The R function cor.test was used to screen for CD58-related genes, and the screening criteria were that the Pearson correlation coefficient was >0.5, and *P*-value was <0.001.

The mean ± standard deviation and frequency or percentage were utilized to present the baseline data for continuous and categorical variables, respectively. The t- and chi-square tests were used to examine the variances between the CD58 expression or risk score groups for continuous and categorical variables, respectively. All the abovementioned analyses were performed in the R statistical environment and Free Statistics analysis platform (Version 1.9, Beijing, China). Statistical significance was determined by a two-sided *P*-value less than 0.05.

2.4. Immunohistochemical test of pathological specimens

This study included thirty two individuals diagnosed with gliomas who received treatment at the Department of Neurosurgery of the First Affiliated Hospital of Jishou University from 2015 to 2020 retrospectively. All patients were treated surgically for the first time and had not undergone any prior treatment. All patients were treated surgically for the first time and had not undergone any prior treatment. Every patient received complete microsurgical removal and was diagnosed with glioma through a joint analysis conducted by two skilled pathologists. Among the patients with glioma, there were 17 males, accounting for 53.1 % of the total, and 15 females,

representing 46.9 %. The age of patients was 43.0 ± 14.0 years. These included 12 WHO II, 10 WHO III, and 10 glioblastoma (GBM) cases. The LGG group consisted of cases with WHO grades II and III, while the GBM group consisted of cases with glioblastoma. Furthermore, eight individuals with traumatic brain injury provided normal brain tissue. Every patient provided normal brain tissue signed the informed consent form, and the study received approval from the hospital's ethics committee (Approval No. EC-2021006). The tissue samples were fixed, embedded, and sectioned. CD58 staining was performed using immunohistochemistry (primary antibody, ab214035, Abcam, USA; secondary antibody, ab6795, Abcam, USA). Images were acquired using the NDP.view 2 microscope and processed using ImageJ software (version 1.51). CD58-positive cells were counted in at least five microscopic fields (200 × magnification) and exhibited as the number of positive cells per 100 cells.

2.5. Cell culture

The U251 and U87 MG cell lines were procured from the American Type Culture Collection (ATCC) located in The Global Bioresource Center in the United States, and the normal human astrocyte line (HEB) was provided by BNCC (BeNa Culture Collection, China). The U87 cell line (catalogue number in ATCC: HTB-14), from a glioblastoma of unknown origin, was authenticatd using STR profiling. The frozen cells in the liquid nitrogen were immediately thawed in a 37 °C water bath and then placed in a culture dish with a diameter of 6 cm. The cells were cultivated in a full medium comprising of 10 % fetal bovine serum under a routine environment.

2.6. Quantitative PCR (qPCR)

qPCR was used to detect the mRNA expression of *CD58* in U251, U87, and HEB cells. Fluorescent quantitative PCR was conducted with a qPCR kit (Thermo Fisher Scientific-CN, A44359, China). PCR reactions were conducted with a total of 35 cycles, using an annealing temperature of 58 °C. The primer sequences for *CD58* were 5′-ATGGTGTTGTGTATGGGAATG-3′ and 5′-ACAAGT-TAGTGTGGGAGATGGA-3′. The β-actin primers were 5′- CCTGTACGCCAACACAGTGC-3′ and 5′-ATACTCCTGCTTGCTGATCC-3′. GeneChem Co., Ltd. (Shanghai, China) generated the primers.

2.7. Transfection

Short hairpin RNA (shRNA) was used to subject U251 and U87 cells to RNA interference (RNAi). *CD58* shRNA (KD) and non-target control (NC) shRNA were synthesized by BGI Genomics (BGI Genomics Co., Ltd., China). For shRNA transfection, 3.2×10^4 U251 or U87 cells were sown in 12-well plates and then grown for 24 h at 37 °C. Upon reaching 80 % confluency, the cells were exposed to lentiviral suspensions containing NC shRNA or CD58 shRNA, and subsequently incubated overnight. Next, the cells were cultured for another 24 h using new medium after removing the lentivirus-containing solution, and then treated with 0.5 μg/mL puromycin for selection. After amplification, the remaining cells were examined under a fluorescence microscope (IX71, Olympus, Japan) to observe the presence of green fluorescent protein (GFP). The cells were collected for subsequent experiments when transfection efficiency and confluency reached 80 %.

2.8. Western blot

Cell lysates from HEB-, U251-, U87-, and shRNA-transfected cells were harvested for Western blot analysis. ShRNA-transfected cells included U251 NC shRNA (U251 NC), U251 *CD58* shRNA (U251 KD), U87 NC shRNA (U87 NC), and U87 *CD58* shRNA (U87 KD) groups. In this study, the following antibodies were used: anti-CD58 from Proteintech (10878-1-AP, USA), β-actin from SANTA CRUZ (sc-69879, USA), mouse and rabbit IgG secondary antibodies, and ECL luminescent solution from CST (#7076, #7074, #7003, USA).

2.9. Cell proliferation assay

The CCK8 reagent (CK04, Dojindo Molecular Technologies, Japan) was utilized to assess the ability of cells to proliferate. U251 and U87 cells (2000 cells/well) from the NC and KD groups were seeded in 96-well plates. 100 μL/well of the CCK-8 solution was added to the plates at designated time intervals (days 1, 2, 3, 4, and 5). Using a microplate reader (Nexcelom Cellometer Auto 2000, USA), the measurement of absorbance at 450 nm was taken for each well. The OD450 values in the NC and KD groups were compared.

2.10. Apoptosis assay

Cells (1.2×10^{12} cells/well) from the NC or KD groups were transplanted into six-well plates. As these cells had 85 % confluence, apoptosis was quantified in each group using the apoptosis detection kit (88–8007, eBioscience, USA) and the FACS apoptosis single-stain assay instrument (BD Accuri™C6 Plus, USA), and the results were analyzed using the FACS Diva software.

2.11. Cell migration assay

A total of 8×10^4 cells/well from either the NC or KD groups were planted into the upper chamber of the transwell chamber (Corning, NY), which contained 100 μL of serum-free DMEM medium. 600 μL of DMEM medium with a concentration of 30 % FBS was added to the lower chamber to induce migration for 16 h. After migrating to the bottom of the upper chamber, cells were immobilized

using 4 % paraformaldehyde and then subjected to staining with 0.5 % crystal violet. In each upper chamber, we selected five fields of view at a magnification of 200 × in a random manner. We counted the quantity of cells in each field and calculated the average values of the five fields.

2.12. Statistical analysis for pathological specimens and cell assays

The data were reported as mean ± SD from a minimum of three separate trials. The Kruskal-Wallis H test and Bonferroni correction were used to determine statistical significance for pathological specimens, while the *t*-test was used for cell assays conducted with IBM SPSS Statistics 24.0 (SPSS, Inc., Chicago, IL, USA). A *P* value less than 0.05 was deemed to represent statistical significance.

2.13. Screening, enrichment analyses, and protein-protein interaction (PPI) for CD58-related genes

The 'Venn' package of R software was utilized to screen 1210 CD58-associated genes by intersecting CD58-related genes in TCGA and CGGA datasets. Enrichment analysis and visualization of gene ontology (GO) and Kyoto Encyclopedia of Genes and Genomes (KEGG) pathways of the CD58-related genes utilized various R software packages, such as 'ClusterProfiler,' 'unprincipled,' 'org.Hs.eg.db,' and 'ggplot 2'. Enrichment was performed using a pvalueFilter of 0.05 and a qvalueFilter of 0.05, and the results was utilized to generate the bubble chart. Enrichment and PPI network analyses were performed using Metascape, a online platform (http://metascape.org/) [32]. We utilized three operational components of Metascape, namely 'Pathway and Process Enrichment Analysis', 'Quality Control and Association Analysis', and 'Protein-protein Interaction Enrichment Analysis'.

2.14. Screening and validating core CD58-related genes

To build a PPI network of CD58-related genes, we utilized the STRING database (www.string-db.org) and set a minimum interaction score of 0.4. Two plugins in the Cytoscape software (V3.8.2), cytoHubba (V0.1), and CytoNCA (V2.1.6), were applied for the centrality analysis of the interaction network [33,34]. Initially, we employed the cytoHubba to identify the foremost 100 central nodes from the PPI network of genes associated with CD58. These 100 hub nodes underwent two rounds of rescreening using the CytoNCA with six distinct centralities: degree (DC), betweenness (BC), eigenvector (EC), closeness (CC), network (NC), and local average connectivity-based method (LAC). The nodes whose values in the six centralities were all greater than the median in the two rounds of screening were identified as additional central nodes, and finally 20 nodes were selected. To further narrow down the core nodes, we used the cytoHubba plugin to filter the top 10 hub nodes from these 20 nodes as alternative core genes. These 10 alternative core genes were intersected with *CD58* related genes in the Rembrandt and GSE16011 datasets to obtain the final six *CD58* related core genes, including caspase 1 *(CASP1),* interleukin-18 *(IL18),* C–C motif chemokine ligand 2 *(CCL2),* protein tyrosine phosphatase receptor type C *(PTPRC),* Myeloid differentiation primary response protein 88 *(MYD88),* and Toll-like Receptor 2 *(TLR2)*.

Validation of these core CD58-associated genes was performed in the previous four glioma datasets, Human Protein Atlas (HPA) database, and CancerSEA (Cancer Single-cell State Atlas) database. Pearson correlation coefficient, KM curve and ROC curve analyses were used to observe the relations of these genes with CD58 and the glioma mortality. The implementation of these three analyses has been provided in the "Data analysis methods used in glioma datasets" section of the Methods. The HPA database, accessible at https://www.proteinatlas.org/, serves as a freely available repository for human proteins [35]. Pathologically stained images of brain cortical and glioma tissues using the same primary antibody were used to visualize the protein levels of these core genes. The antibodies for CASP1, CCL2, IL18, MYD88, and PTPRC are HPA003056, CAB013676, CAB007772, CAB009104, and CAB080251, respectively. Pathologic staining results of TLR2 in the HPA database are missing and therefore not shown. CancerSEA is a dedicated database that aims to comprehensively decode distinct functional states of cancer cells at single-cell resolution [36]. The URL is http://biocc.hrbmu.edu.cn/CancerSEA/. CancerSEA was uesd to validate the expression and subcellular localization of these six core genes in various glioma single-cell transcriptome datasets. The GBM-010-02-1A dataset in CancerSEA was used to demonstrate the subcellular localization of *CD58* and its core associated genes. This dataset was selected because it has the highest number of cells in the 10X genomics scRNA-Seq datasets.

3. Results

3.1. Pan-cancer analysis of CD58

As displayed in Supplementary fig. 1, *CD58* expressed in 31 kind of normal tissues. Neural tissues exhibited low level of *CD58* expression. *CD58* exhibited significant upregulation ($p < 0.05$) in 19 tumors, including gliomas, when compared to the control group (Supplementary fig. 1B). Furthermore, it was discovered that elevated levels of CD58 expression were associated with unfavorable prognosis in seven different cancer types, including glioblastoma ($p < 0.05$) (Supplementary fig. 1C).

As indicated in Supplementary table 1, gliomas along with 10 other tumors exhibited a significant association between *CD58* expression and the DNA stemness score (DNAss). As shown in Supplementary table 2 and it was evident that there was a noteworthy association between the three immune infiltration scores (stromal, immune, and ESTIMATE) and *CD58* expression in 14 tumors, including glioma *(*$P < 0.05$).

3.2. Association between CD58 expression and glioma histology and prognosis

The results from the baseline data (Supplementary table 3) showed that the *CD58* high expression group was older, had more cases of GBM and WHO III/IV, and resulted in more deaths and a shorter overall survival. The results from the distribution analysis, KM curve, and ROC curve further supported this trend exhibited by the baseline data (Fig. 2). CD58 was higher in the GBM group, high-expression *CD58* group was with worse prognosis, and *CD58* expression was a good predictor for glioma mortality. These results were consistent in TCGA and CGGA datasets.

The findings from the univariate and multivariate Cox regression analyses indicated that the *CD58* expression category, along with age, histology, and grade, were identified as autonomous predictors of mortality in glioma patients (Supplementary table 4). By adjusting for different covariates, we constructed three models to examine the correlation between *CD58* expression and glioma mortality. The crude model was not adjusted, Model I was modified for age and sex, and Model II was modified for grade based on Model I (Table 1). In the three models of the TCGA dataset, the risk of death in high *CD58* group was increased by 5.45-, 6.29-, and 2.67-fold, respectively, compared with the low *CD58* group (Crude Model: HR = 6.45, 95 % CI: 4.45–9.35; Model I: HR = 7.29, 95 % CI: 4.88–10.89; Model II: HR = 3.67, 95 % CI: 2.23–5.76). Models for the CGGA dataset presented similar results [Crude Model, HR (95 % CI):3.27 (2.69–3.98); Model I, HR (95 % CI):3.17 (2.6–3.86); Model II, HR (95 % CI):2.11 (1.7–2.61)].

Additionally, a subgroup analysis was conducted to assess the consistency of the association between *CD58* expression and glioma

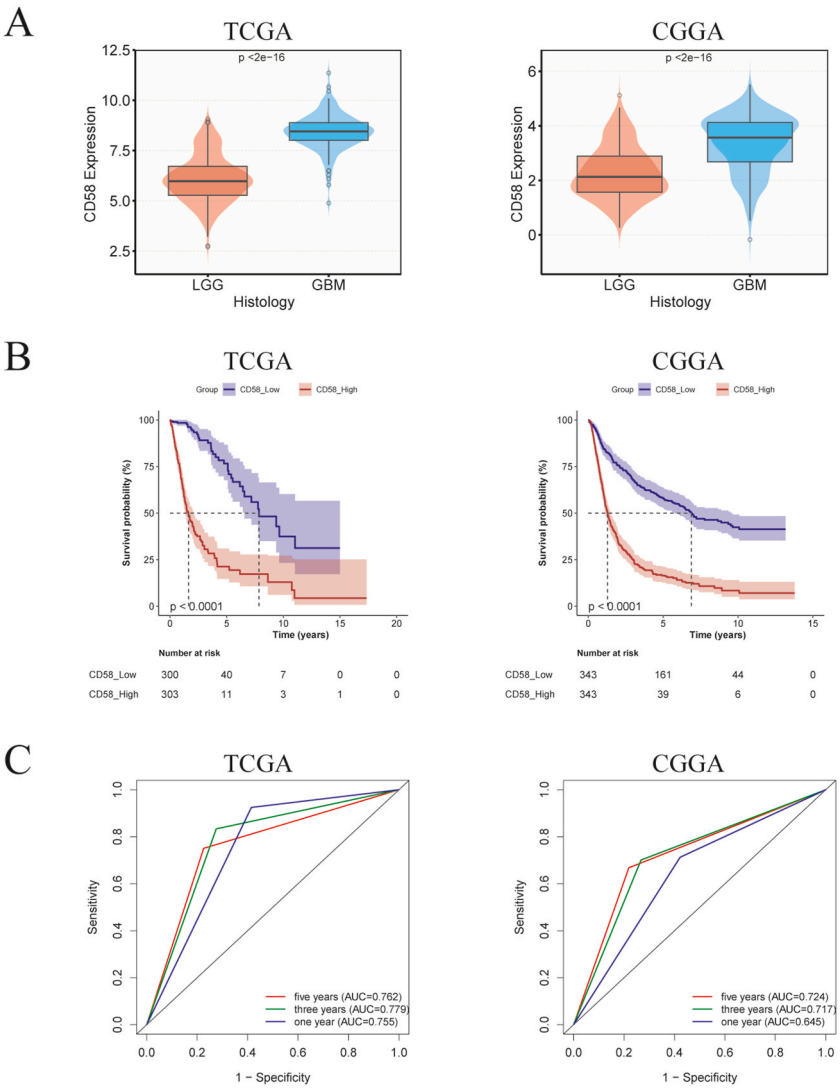

Fig. 2. mRNA expression and prognosis effect of *CD58* in TCGA and CGGA databases. (A) CD58 expression in LGG and GBM groups. (B) KM curves. (C) Time-dependent ROC curves. CD58 expression was higher in GBM groups compared to LGG groups. High CD58 expression was associated with a poorer prognosis, and CD58 grouping showed predictive value for the survival rate of glioma patients. These findings were coherent across the TCGA and CGGA databases.

Table 1
Correlation of *CD58* expression groups with glioma prognosis in TCGA and CGGA databases.

Database	Crude Model		Model I		Model II	
	HR (95%CI)	*P* Value	HR (95%CI)	*P* Value	HR (95%CI)	*P* Value
TCGA	6.45 (4.45–9.35)	<0.001	7.29 (4.88–10.89)	<0.001	3.67 (2.33–5.78)	<0.001
CGGA	3.27 (2.69–3.98)	<0.001	3.17 (2.6–3.86)	<0.001	2.11 (1.7–2.61)	<0.001

Notes: crude model was the non-adjusted model. Model I was adjusted for age and gender. Model II was adjusted for Model I plus histology and grade.

mortality. The total population was classified into subgroups according to age, sex, and histology. The correlation between *CD58* expression and mortality was measured separately for each subpopulation. As shown in Supplementary fig. 2, high *CD58* expression increased the risk of death and this correlation was stable in different subpopulations. No variables interacted with *CD58* expression. These results are consistent in the TCGA and CGGA databases.

3.3. Correlation between the expression of CD58 protein and the pathological grade of glioma samples

Results of immunohistochemical assays (Fig. 3 A–D) showed varied expression of CD58 in the LGG and GBM groups. The cell membrane and cytoplasm were the only locations where CD58 staining was observed, which showed yellow or brownish yellow staining under light microscopy. The findings of the data analysis (Fig. 3E) demonstrated that CD58 expression was higher in the GBM group compared to the LGG group, and lower in the non-tumor brain tissue group compared to the glioma groups.

3.4. Interference with CD58 expression in glioma cells and consequent changes in cellular functions

According to the results of qPCR and Western blot Western blot analysis, it was observed that the glioma cell lines U251 and U87 exhibited elevated CD58 expression compared to the normal astrocyte cell line, HEB (Fig. 4 A–B). An assay of shRNA-mediated knockdown of *CD58* was to understand the mechanism of *CD58* in glioma progression. Intracellular GFP fluorescence and Western

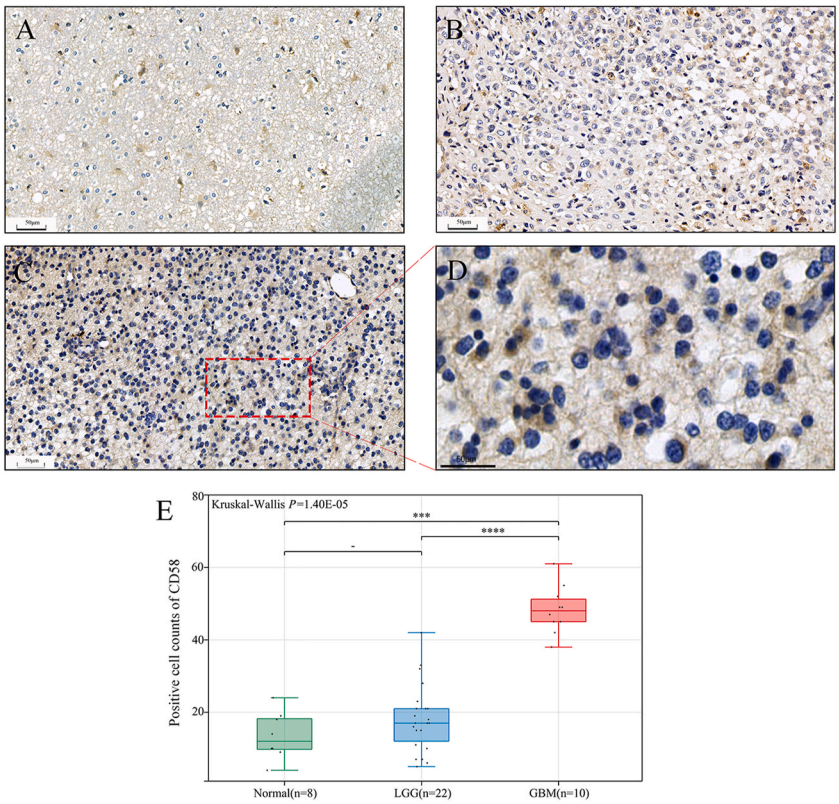

Fig. 3. *CD58* protein expression in normal brain and glioma tissues using immunochemistry. (A) The IHC staining of CD58 in normal brain (200 ×). (B) The IHC staining of CD58 in LGG (200 ×). (C) The IHC staining of CD58 in GBM (200 ×). (D) Microscopic focal magnification views in GBM (400 ×). (E) Analysis of the number of CD58 positive cells in brain and gliomas ($^{-}P > 0.05$, ***$P < 0.001$, ****$P < 0.0001$). Bar represented 100 μm. The expression of CD58 protein was found to be markedly higher in the GBM group compared to both the normal group and the LGG group.

blot were used to confirm lentivirus-mediated shRNA transfection (Fig. 4 C–D). The *CD58* KD group exhibited notably reduced protein level compared to the NC group.

Functional changes in the glioma cells were then examined. Results from CCK8 assay revealed slower cell proliferation was in the KD group than the NC group (Fig. 5A). Results from flow cytometry assessment exhibited the percentage of apoptotic cells was higher in the KD group (Fig. 5B). Results from transwell assay showed migrated cell number in the KD group considerably reduced (Fig. 5 C–D). These findings implied that *CD58* has a considerable influence on the cell proliferation, death, and migration.

3.5. Screening, enrichment analyses, and PPI for CD58-related genes

1210 *CD58*-related genes were identified by screening the overlap between *CD58*-related genes in the TCGA and CGGA datasets (Fig. 6A). Then *CD58* related genes underwent functional enrichment and analysis of protein interaction networks.

The R software was used to carry out GO and KEGG enrichment analyses, presented in Fig. 6B and C, respectively. The focus of biological process (BC) pathways was on the regulation of cell–cell adhesion, cytokine-mediated signaling pathways, and T cell activation. The focus of enriched cellular components (CC) was on extracellular matrix and lumen. Enriched molecular functions (MF) included GTPase, cytokine binding, and immune receptor activity. The KEGG pathways focused on numerous infections, phagosomes, cancer proteoglycans, and apoptosis.

Functional enrichment and PPI analyses were conducted using the Metascape database. As illustrated in Fig. 6 D–F, the pathways *CD58*-related genes focusing on were semblable to those in the R platform. Fig. 6G shows the enrichment analysis of transcription factor (TF) targets. Interferon regulatory factor (*IRF)* Q6, interferon consensus sequence-binding protein (*ICSBP)* Q6, signal transducer

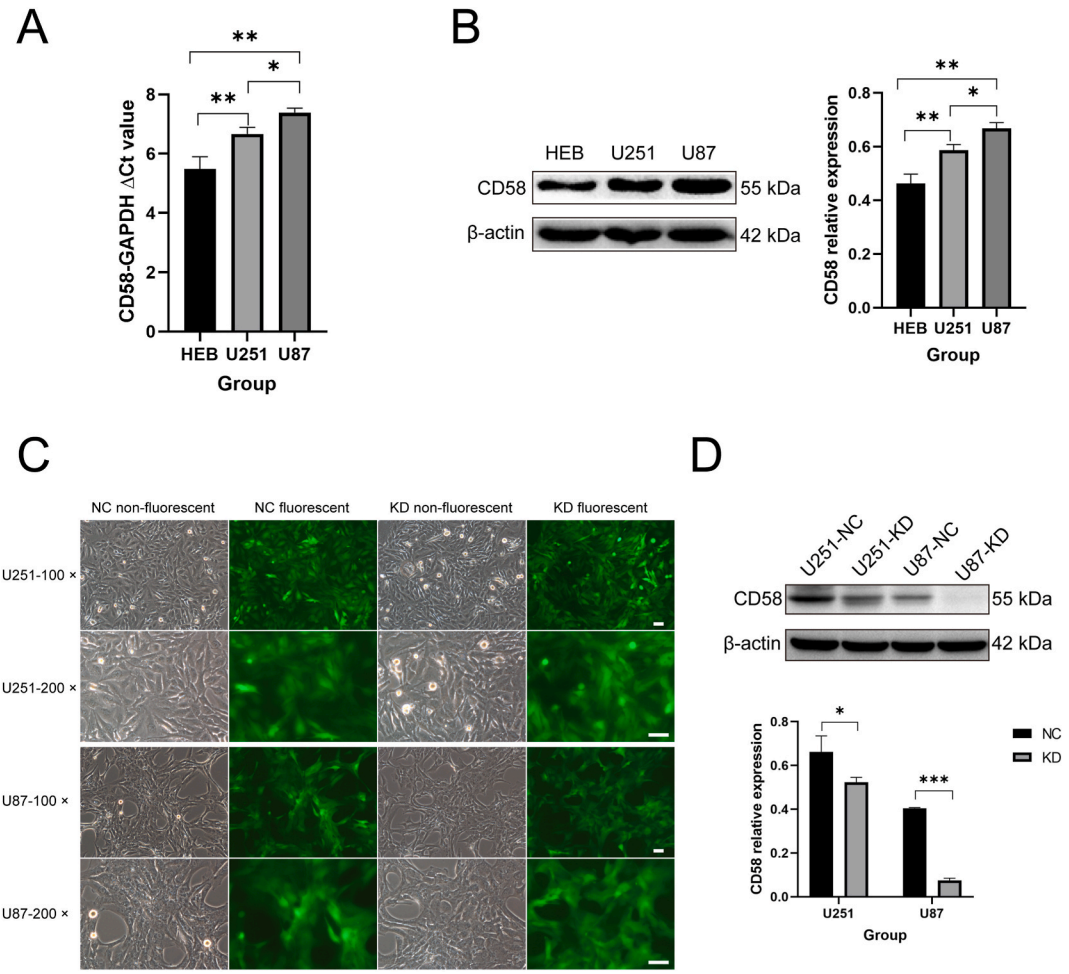

Fig. 4. shRNA interference cells screening and confirmation of transfection effect. (A) and (B) displayed qPCR and Western blot detection of *CD58* expression in HEB, U251, and U87, respectively. (C) Images of cells after shRNA interference. Bar represented 100 μm. (D) *CD58* protein expression in different shRNA interference groups. Results of qPCR and Western blot showed that U251 and U87 cells were suitable for shRNA interference. The fluorescence staining results showed successful transfection. Compared to the blank transfection group (NC), the *CD58* expression was significantly downregulated in the *CD58* shRNA transfection group (KD).

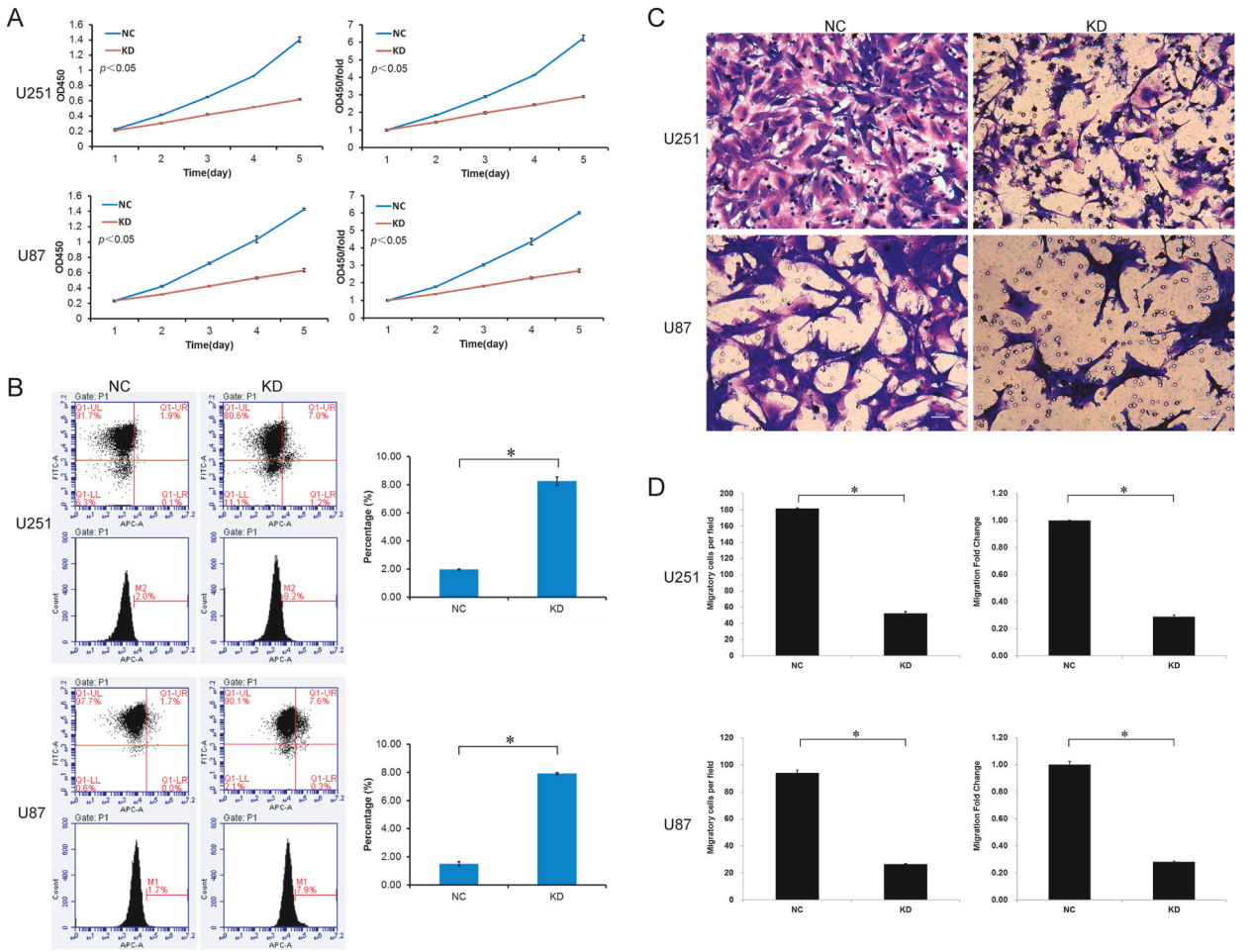

Fig. 5. Functional changes of U251 and U87 cells after *CD58* interference. (A) Cell proliferation assay. Left: OD values at separate time points. Right: OD values relative to day 1. (B) Apoptosis assay. Left: results of flow cytometry. Right: statistical analysis of the flow cytometry results. (C) Cell migration experiments (200 ×). Bar represented 100 μm. (D) Analysis of cell migration experiment results. Left: migrated cell number. Right: migrated cell number relative to the NC group. The *CD58* KD groups showed slower cell proliferation, increased apoptosis and decreased migration compared with the NC groups.

and activator of transcription (*STAT*)5B 01, *STAT5A* 01, and nuclear factor kappa-B (*NFKB)* 01 ranked among the top five terms. Fig. 6H shows the TFs enriched in the TRRUST database. The top five TFs were *NFKB1,* RELA proto-oncogene *(RELA), STAT1,* Class II major histocompatibility complex transactivator (*CIITA)* and *IRF1*. These enriched transcription factors may play essential roles in regulating *CD58*-related genes.

3.6. Screening and validation of core CD58-related genes

Ten alternative core genes in *CD58*-related genes were screened using Cytoscape software (Fig. 6I–L). These 10 candidate core genes were intersected with *CD58* related genes from the Rembrandt and GSE16011 datasets to obtain the final six *CD58* related core genes, including *CASP1, CCL2, IL18, MYD88, PTPRC,* and *TLR2* (Fig. 6M).

Subsequently, we observed *CD58* correlation coefficient, distribution, prognostic impact of *CD58*-related genes in the TCGA and CGGA. As displayed in Supplementary figs. 3 and 4, the six core genes showed a significant positive correlation with *CD58* expression and exhibited higher levels in the GBM group compared to the LGG group. Higher expression of these core *CD58*-related genes predicted a poor prognosis.

We further validated the features of core *CD58*-related genes in the Rembrandt and GSE16011. The outcomes were consistent with those from TCGA and CCGA (Supplementary figs. 5 and 6). These results suggest that these six core *CD58*-related genes may play a significant role in glioma progression, which is affected by *CD58*.

Furthermore, the HPA database was utilized to validate the protein expression of these central genes in both normal cerebral cortical tissues and gliomas (Supplementary fig. 7). Compared to normal brain tissue, the expressions of CASP1, IL18, and MYD88 were upregulated in gliomas, whereas there was no significant differences in the expression of CCL2 and PTPRC between the two groups.

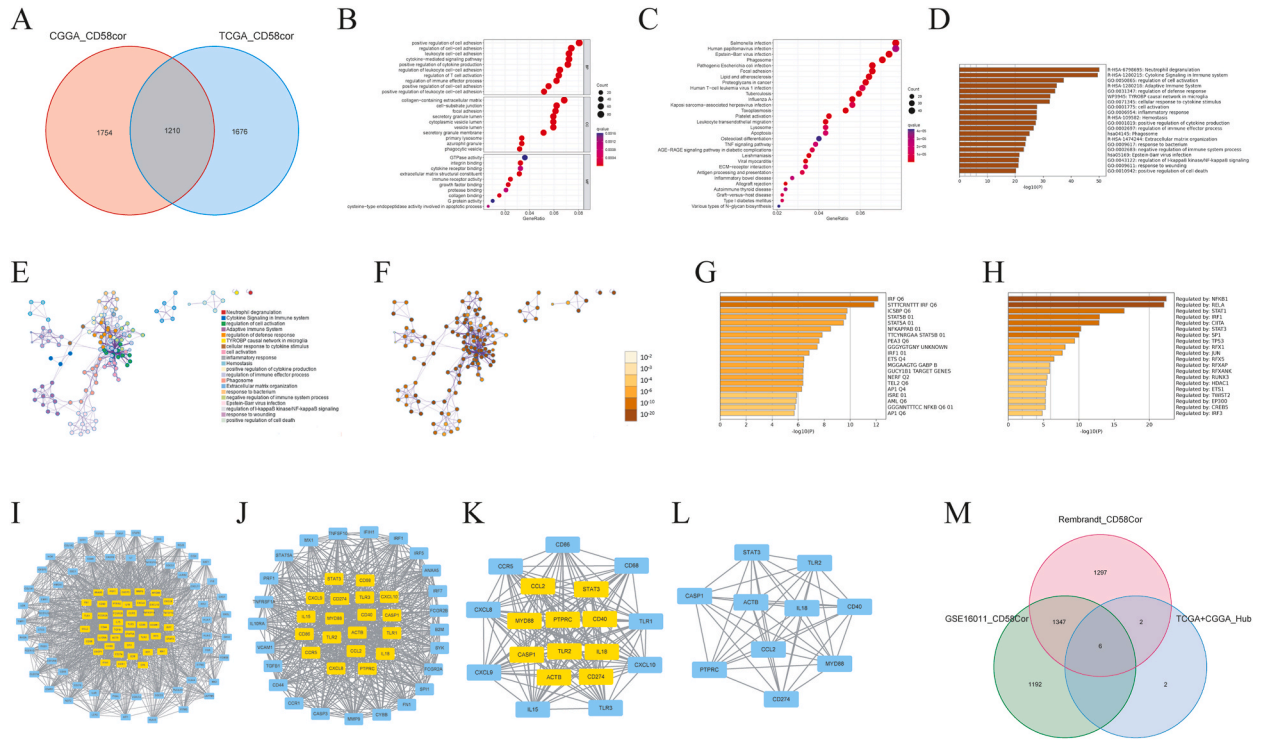

Fig. 6. Screening for *CD58*-related gene clusters and core genes. (A) *CD58*-related gene clusters screened by the intersection of *CD58*-related genes in TCGA and in CGGA. (B) and (C) showed GO enrichment and KEGG enrichment analysis of *CD58*-related gene groups with R software packages, respectively. (D)–(H) showed enrichment analysis and PPI of *CD58*-related gene groups at Metascape. (D)Bar graph, colored by *P*-values. (E) Network of enriched terms, colored by cluster ID. (F) Network of enriched terms, colored by *P*-value. (G) Overview of enrichment analysis in Transcription-Factor-Targets. (H) Overview of the enrichment analysis in TRRUST. (I)–(L) showed the screening of alternative core related genes. (M) Identification of core *CD58*-related genes using Rembrandt and GSE16011 datasets. 1210 *CD58*-related genes were screened from TCGA and CGGA datasets. *CD58*-related genes were primarily engaged in promoting leukocyte cell–cell adhesion, signaling pathways mediated by cytokines, regulating T cell activation, neutrophil degranulation, the adaptive immune system, regulating defense responses, and inflammatory responses. Regulatory factors for these *CD58*-related genes were *IRF1, ICSBP, STAT5, NFKB1, PEA3, RELA, STAT1, CIITA, STAT3, SP1, TP53,* among others. Ten candidate core genes were obtained after four rounds of screening via CytoScape. The intersection of these 10 genes with *CD58*-related genes from Rembrandt and GSE16011 datasets finally identified six related core genes, which were *CASP1, CCL2, IL18, MYD88, PTPRC,* and *TLR2*.

Pathologic staining results of TLR2 in the HPA database are missing and therefore not shown.

At last, we validated the expression and subcellular localization of the six core genes in the glioma single-cell transcriptome dataset by CanceSEA. As shown in Supplementary figs. 8–9, *CD58* and its 6 core related genes were expressed in different glioma single cell databases. In terms of cellular subpopulation localization (GBM-010-02-1A dataset), all core genes and *CD58* were highly expressed in monocytes except for *TLR2. TLR2*, on the other hand, was mainly expressed in dendritic cells and macrophages.

3.7. Correlation of the signature of CD58 & core-related genes with glioma type and prognosis

Risk scores for the signatures of *CD58* and core-related genes in the four datasets were applied to observe the association of *CD58* and core-related genes with glioma typing and prognosis.

The results from the baseline data (Supplementary table 5) showed that the high-risk groups were older, had more cases of GBM and WHO III/IV, resulted in more deaths, and had shorter overall survival. These results are similar to those observed in the *CD58* group. The results of the distribution analysis, KM curves, and ROC curves in Fig. 7 also coincided with the trends exhibited by the baseline data. Notably, these results are consistent among the four datasets, which increases the credibility of the results.

After adjusting for different covariates, we constructed two Cox regression models to examine the association between different risk groups and glioma mortality for each dataset. The crude models were not adjusted, whereas the adjusted models were modified for age, sex, histology, and grade (Table 2). The high risk group had a 6.49-, 2.82-, 1.72-, and 4.23-fold increased risk of death in the four datasets, respectively, compared with the low risk group [HR (95 % CI). TCGA: 7.49 (5.14–10.93); CGGA: 3.82 (3.13–4.66); Rembrandt: 2.72 (1.99–3.71); GSE16011: 5.23 (3.49–7.84)]. The adjusted models exhibited similar results [HR (95 % CI). TCGA: 3.21 (2.06–5.01); CGGA: 2.45 (1.96–3.06); Rembrandt:1.64 (1.15–2.35); GSE16011: 4.6 (2.6–8.16)], which suggests that the correlation between risk score group and glioma mortality is stable.

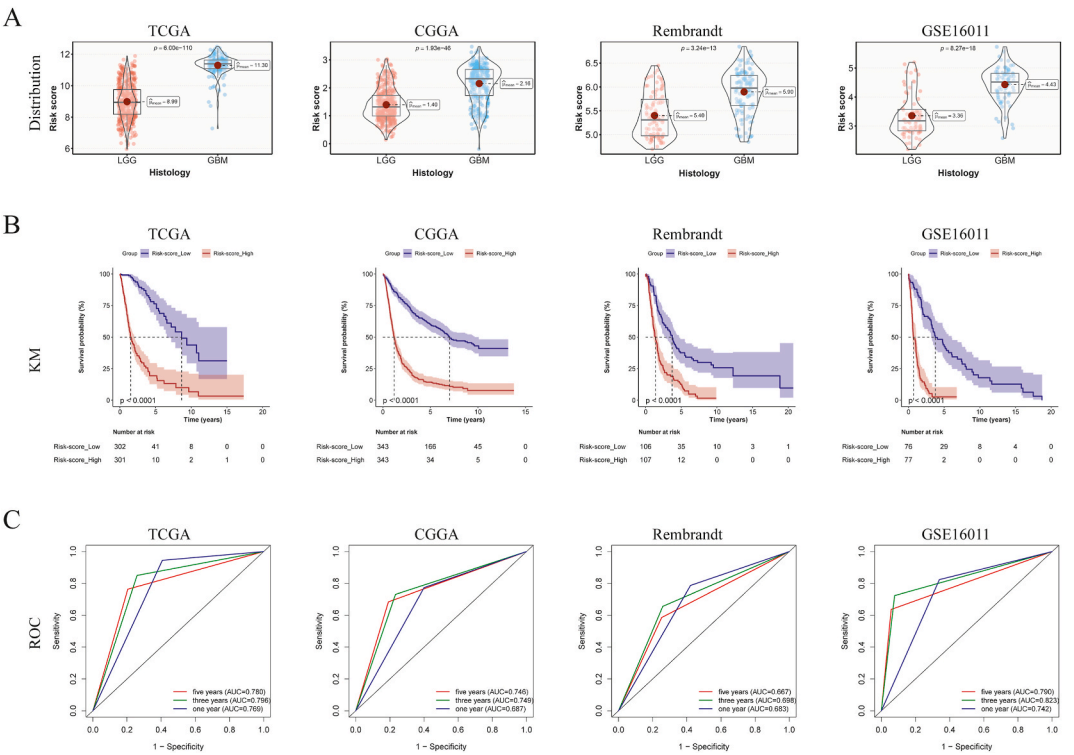

Fig. 7. Distribution and prognosis effect of risk score from the signature of *CD58* and core *CD58*-related genes in the four databases. (A) The risk score distribution in LGG groups and GBM groups. (B) Kaplan–Meier curves. (C) Time-dependent ROC curves. Risk score was higher in GBM groups than LGG groups. The higher risk score predicted worse prognosis. The risk score has the capability to predict the survival rate of patients with glioma. These results were consistent across all the four databases.

Table 2
Correlation of the groups of risk score from *CD58* & core-related genes with glioma prognosis in four databases.

Database	Crude Model		Adjusted Model	
	HR (95%CI)	*P* Value	HR (95%CI)	*P* Value
TCGA	7.49 (5.14–10.93)	<0.001	3.21 (2.06–5.01)	<0.001
CGGA	3.82 (3.13–4.66)	<0.001	2.45 (1.96–3.06)	<0.001
Rembrandt	2.72 (1.99–3.71)	<0.001	1.64 (1.15–2.35)	0.006
GSE16011	5.23 (3.49–7.84)	<0.001	4.6 (2.6–8.16)	<0.001

Notes: crude model was the non-adjusted model. Adjusted Model was adjusted for age, gender, histology and grade.

4. Discussion

During this investigation, it was discovered that elevated levels of *CD58* indicated more aggressive glioma subtypes and a poorer prognosis. Conversely, reduced *CD58* expression correlated with decreased cell proliferation, increased apoptosis, and diminished glioma cell metastasis. Potential pathways involved in *CD58*-related effects were enriched in immune cell adhesion and immune factor activation, and the signature of *CD58* and its core related genes had good predictive power for glioma prognosis.

The findings from the pan-cancer investigation revealed that *CD58* expression was elevated in various tumors, and this upregulation was linked to an unfavorable prognosis. Meanwhile, *CD58* expression exhibited a positive association with DNAss and immune infiltration. These results align with other research on *CD58*, indicating that *CD58* could potentially serve as a universal biomarker for cancers [17–20].

When focusing on glioma-related *CD58* research, we studied it from three perspectives: bioinformatics databases, clinical samples, and cell models. The results from these three aspects were consistent. The pathway of *CD58*-related gene enrichment was also extremely consistent with the function of *CD58* in the immune system, which further reflects the affect of the immune system on the occurrence and development of gliomas [37].

Similarly, the core genes screened from *CD58* related genes are closely linked with gliomas. *MYD88* and *CASP1* participate in immunogenic cell death in LGG [38]. Polarized bone marrow-derived macrophages could upregulate *CCL2* and induce glioblastoma cell migration [39]. The occurrence of glioma is significantly associated with *IL-18* gene variations and levels of expression [40]. *IL8*

and *PTPRC* are highly expressed in LGG and are independent prognostic factors of LGG [41]. The impairment of microglia induced by *TLR2* inhibits the growth and stimulation of $CD4^+$ T cells, which helps glioma evade the immune system [42]. And *TLR2* also promotes glioma development and progression by enhancing autopha. These results are in agreement with ours, suggesting that screening *CD58* related core genes with bioinformatics is feasible [43].

In addition to the *CD58*-related genes discovered in this study, other signaling molecules are also involved in the tumor immune regulation of *CD58*. *CD58* may function as an *NF-κB* binding site in glioma progression [26]. CD58 and soluble CD58 induce migration, self-renewal, and pluripotency of liver cancer cells in vitro, possibly through the *AKT/GSK-3β/*β-catenin signaling pathway [44]. Blinatumomab is an effective immunotherapeutic agent for B-cell acute lymphoblastic leukemia. Loss of *CD19* or *CD58* is a major driver of Blinatumomab resistance. Loss of *CD58* eliminates Blinatumomab-induced T-cell activation [45]. $CD58^{-}CD2$ axis deficiency promotes immune escape of melanoma cells by reducing T-cell activation, tumor-infiltrating T-cell proliferation, and impairing PD-L1 protein stability [46]. The presence of Marvel transmembrane domain-containing 6 (*CMTM6*), a positive regulator and molecular partner of *PD-L1*, positively regulates *CD58* expression as well. *CMTM6* interacts with *CD58* and *PD-L1*, maintaining the expression of these two immunosuppressive ligands with opposite functions. The presence of *CMTM6* and *CD58* on different tumor cells significantly affects the T-cell-tumor interaction and response to PD-L1-PD-1 blockade [47]. Taken together, these findings demonstrate the multifaceted and complex role of *CD58* in tumor immunity.

Still, our study has a few limitations: 1) the absence of a primary glioma cell model; 2) incomplete cell experiments; 3) insufficient research on the mechanisms of *CD58* action; 4) limited diversity in the methods of biological information analysis and presentation; 5) a lack of experiments targeting the core gene cluster associated with *CD58*. We will incorporate additional basic experiments and expand the scope of bioinformatics analysis in future researches to provide a more comprehensive understanding of the mechanisms and functions of *CD58* in gliomas.

5. Conclusion

Collectively, these findings indicate that elevated *CD58* levels are linked to more malignant glioma subtypes and serve as an autonomous predictor for glioma mortality. *CD58* and its core-related genes could potentially function as innovative indicators for the detection and management of gliomas.

Ethics approval and consent to participate

The Ethics Committee of the First Affiliated Hospital of Jishou University reviewed and granted approval for this study (Approval No. EC-2021006). Glioma paraffin samples were collected retrospectively, so informed consent could not be obtained from patients. Each traumatic brain injury patient who provided a normal specimen of brain tissue signed an informed consent form.

Funding

This research was funded by the Natural Science Foundation of China (Nos. 81,560,414 and 82,160,554) and the program of the Hunan Provincial Health Commission (No. 20201191 and 20230451).

Data availability

This published article contains all the data that was produced or examined during the study.

CRediT authorship contribution statement

Zhi Tian: Writing – original draft, Funding acquisition, Data curation. **Wei Jia:** Data curation, Writing – original draft, Formal analysis. **Zhao Wang:** Methodology, Data curation. **Hui Mao:** Methodology, Data curation. **Jingjing Zhang:** Methodology, Data curation. **Qiongya Shi:** Methodology, Data curation. **Xing Li:** Methodology, Data curation. **Shaoyu Song:** Methodology, Data curation. **Jiao Zhang:** Methodology, Data curation. **Yingjie Zhu:** Methodology, Data curation. **Bo Yang:** Resources, Methodology. **Chunhai Huang:** Conceptualization, Supervision, Funding acquisition. **Jun Huang:** Resources, Funding acquisition, Conceptualization.

Declaration of competing interest

The authors declare that they have no known competing financial interests or personal relationships that could have appeared to influence the work reported in this paper.

Acknowledgements

We extend our gratitude to all the participants for their generous donation of samples.

Appendix A. Supplementary data

Supplementary data to this article can be found online at https://doi.org/10.1016/j.heliyon.2024.e29275.

References

[1] K. Zhang, et al., Clinical management and survival outcomes of patients with different molecular subtypes of diffuse gliomas in China (2011-2017): a multicenter retrospective study from CGGA, Cancer Biol Med 19 (10) (2022) 1460–1476, https://doi.org/10.20892/j.issn.2095-3941.2022.0469.
[2] N. Kumar, et al., Impact of Immunohistochemical profiling of Glioblastoma multiforme on clinical outcomes: real-world scenario in resource limited setting, Clin. Neurol. Neurosurg. 207 (2021) 106726, https://doi.org/10.1016/j.clineuro.2021.106726.
[3] T. Jiang, et al., Clinical practice guidelines for the management of adult diffuse gliomas, Cancer Lett. 499 (2021) 60–72, https://doi.org/10.1016/j.canlet.2020.10.050.
[4] S. Watkins, S. Robel, I.F. Kimbrough, S.M. Robert, G. Ellis-Davies, H. Sontheimer, Disruption of astrocyte-vascular coupling and the blood-brain barrier by invading glioma cells, Nat. Commun. 5 (2014) 4196.
[5] A. Louveau, I. Smirnov, T.J. Keyes, et al., Structural and functional features of central nervous system lymphatic vessels, Nature 523 (7560) (2015) 337–341.
[6] C. Yang, K.E. Hawkins, S. Doré, E. Candelario-Jalil, Neuroinflammatory mechanisms of blood-brain barrier damage in ischemic stroke, Am. J. Physiol. Cell Physiol. 316 (2) (2019) C135–C153.
[7] Y. Qi, B. Liu, Q. Sun, X. Xiong, Q. Chen, Immune checkpoint targeted therapy in glioma: status and hopes, Front. Immunol. 11 (2020) 578877.
[8] M. Noguchi, T. Sasada, K. Itoh, Personalized peptide vaccination: a new approach for advanced cancer as therapeutic cancer vaccine, Cancer Immunol. Immunother. 62 (5) (2013) 919–929.
[9] L.C. Chen, H.Y. Zhang, Z.Y. Qin, et al., Serological identification of URGCP as a potential biomarker for glioma, CNS Neurosci. Ther. 20 (4) (2014) 301–307.
[10] A. Desjardins, M. Gromeier, J.E. Herndon 2nd, et al., Recurrent glioblastoma treated with recombinant poliovirus, N. Engl. J. Med. 379 (2) (2018) 150–161.
[11] L.M. Liau, K. Ashkan, D.D. Tran, et al., First results on survival from a large Phase 3 clinical trial of an autologous dendritic cell vaccine in newly diagnosed glioblastoma, J. Transl. Med. 16 (1) (2018) 142.
[12] Y. Yao, F. Luo, C. Tang, et al., Molecular subgroups and B7-H4 expression levels predict responses to dendritic cell vaccines in glioblastoma: an exploratory randomized phase II clinical trial, Cancer Immunol. Immunother. 67 (11) (2018) 1777–1788.
[13] N. Hilf, S. Kuttruff-Coqui, K. Frenzel, et al., Actively personalized vaccination trial for newly diagnosed glioblastoma, Nature 565 (7738) (2019) 240–245.
[14] D.B. Keskin, A.J. Anandappa, J. Sun, et al., Neoantigen vaccine generates intratumoral T cell responses in phase Ib glioblastoma trial, Nature 565 (7738) (2019) 234–239.
[15] L. Osborn, E.S. Day, G.T. Miller, et al., Amino acid residues required for binding of lymphocyte function-associated antigen 3 (CD58) to its counter-receptor CD2, J. Exp. Med. 181 (1) (1995) 429–434.
[16] Y. Zhang, Q. Liu, S. Yang, Q. Liao, CD58 immunobiology at a glance, Front. Immunol. 12 (2021) 705260.
[17] S. Xu, Z. Wen, Q. Jiang, et al., CD58, a novel surface marker, promotes self-renewal of tumor-initiating cells in colorectal cancer, Oncogene 34 (12) (2015) 1520–1531.
[18] Y. Zhang, Q. Liu, J. Liu, Q. Liao, Upregulated CD58 is associated with clinicopathological characteristics and poor prognosis of patients with pancreatic ductal adenocarcinoma, Cancer Cell Int. 21 (1) (2021) 327.
[19] Y. Shen, J.S. Eng, F. Fajardo, et al., Cancer cell-intrinsic resistance to BiTE therapy is mediated by loss of CD58 costimulation and modulation of the extrinsic apoptotic pathway, J Immunother Cancer 10 (3) (2022).
[20] Y. Xiong, H. Motomura, S. Tamori, et al., High expression of CD58 and ALDH1A3 predicts a poor prognosis in basal-like breast cancer, Anticancer Res. 42 (11) (2022) 5223–5232.
[21] A. Mäenpää, P.E. Kovanen, A. Paetau, J. Jääskeläinen, T. Timonen, Lymphocyte adhesion molecule ligands and extracellular matrix proteins in gliomas and normal brain: expression of VCAM-1 in gliomas, Acta Neuropathol. 94 (3) (1997) 216–225, https://doi.org/10.1007/s004010050696.
[22] K. Rössler, C. Neuchrist, K. Kitz, O. Scheiner, D. Kraft, H. Lassmann, Expression of leucocyte adhesion molecules at the human blood-brain barrier (BBB), J. Neurosci. Res. 31 (2) (1992) 365–374, https://doi.org/10.1002/jnr.490310219.
[23] M.C. Kuppner, M.F. Hamou, N. de Tribolet, Activation and adhesion molecule expression on lymphoid infiltrates in human glioblastomas, J. Neuroimmunol. 29 (1–3) (1990) 229–238, https://doi.org/10.1016/0165-5728(90)90166-k.
[24] S. Sarkar, A. Ghosh, J. Mukherjee, S. Chaudhuri, S. Chaudhuri, CD2-SLFA3/T11TS interaction facilitates immune activation and glioma regression by apoptosis, Cancer Biol. Ther. 3 (11) (2004) 1121–1128, https://doi.org/10.4161/cbt.3.11.1214.
[25] J. Mukherjee, et al., T11TS/S-LFA3 induces apoptosis of the brain tumor cells: a new approach to characterise the apoptosis associated genetic changes by arbitrarily primed-PCR, Cancer Lett. 222 (1) (2005) 23–38, https://doi.org/10.1016/j.canlet.2004.09.014.
[26] E. Vartholomatos, et al., An NF-κB- and therapy-related regulatory network in glioma: a potential mechanism of action for natural antiglioma agents, Biomedicines 10 (5) (2022) 935, https://doi.org/10.3390/biomedicines10050935.
[27] M. Wu, Y. Chen, G. Hua, L. Chunhui, The CD2-CD58 axis: a novel marker predicting poor prognosis in patients with low-grade gliomas and potential therapeutic approaches, Immunity Inflammation and Disease 11 (10) (2023) e1022, https://doi.org/10.1002/iid3.1022.
[28] W. Shen, Z. Song, X. Zhong, et al., Sangerbox: a comprehensive, interaction-friendly clinical bioinformatics analysis platform, iMeta 1 (3) (2022) e36, 2022.
[29] Z. Zhao, F. Meng, W. Wang, Z. Wang, C. Zhang, T. Jiang, Comprehensive RNA-seq transcriptomic profiling in the malignant progression of gliomas, Sci. Data 4 (2017) 170024.
[30] X. Liu, Y. Li, Z. Qian, et al., A radiomic signature as a non-invasive predictor of progression-free survival in patients with lower-grade gliomas, Neuroimage Clin 20 (2018) 1070–1077.
[31] L.A. Gravendeel, et al., Intrinsic gene expression profiles of gliomas are a better predictor of survival than histology, Cancer Res. 69 (23) (2009) 9065–9072, https://doi.org/10.1158/0008-5472.CAN-09-2307.
[32] Y. Zhou, B. Zhou, L. Pache, et al., Metascape provides a biologist-oriented resource for the analysis of systems-level datasets, Nat. Commun. 10 (1) (2019) 1523.
[33] C.H. Chin, S.H. Chen, H.H. Wu, C.W. Ho, M.T. Ko, C.Y. Lin, cytoHubba: identifying hub objects and sub-networks from complex interactome, BMC Syst. Biol. 8 (Suppl 4) (2014) S11. Suppl 4.
[34] Y. Tang, M. Li, J. Wang, Y. Pan, F.X. Wu, CytoNCA: a cytoscape plugin for centrality analysis and evaluation of protein interaction networks, Biosystems 127 (2015) 67–72.
[35] M. Uhlén, et al., Proteomics. Tissue-based map of the human proteome, Science 347 (6220) (2015) 1260419, https://doi.org/10.1126/science.1260419.
[36] H. Yuan, et al., CancerSEA: a cancer single-cell state atlas, Nucleic Acids Res. 47 (D1) (2019) D900–D908, https://doi.org/10.1093/nar/gky939.
[37] X. Mao, J. Xu, W. Wang, et al., Crosstalk between cancer-associated fibroblasts and immune cells in the tumor microenvironment: new findings and future perspectives, Mol. Cancer 20 (1) (2021) 131.
[38] J. Cai, Y. Hu, Z. Ye, et al., Immunogenic cell death-related risk signature predicts prognosis and characterizes the tumour microenvironment in lower-grade glioma, Front. Immunol. 13 (2022) 1011757.
[39] L. Wu, W. Wu, J. Zhang, et al., Natural coevolution of tumor and immunoenvironment in glioblastoma, Cancer Discov. 12 (12) (2022) 2820–2837.
[40] Y. Yang, Y.J. Song, Q.B. Nie, Y.F. Wang, M. Zhang, G.S. Mao, Correlations of IL-18 and IL-6 gene polymorphisms and expression levels with onset of glioma, Eur. Rev. Med. Pharmacol. Sci. 26 (5) (2022) 1475–1483.

[41] Y. He, Z. Lin, S. Tan, Identification of prognosis-related gene features in low-grade glioma based on ssGSEA, Front. Oncol. 12 (2022) 1056623.
[42] J. Qian, F. Luo, J. Yang, et al., TLR2 promotes glioma immune evasion by downregulating MHC Class II molecules in microglia, Cancer Immunol. Res. 6 (10) (2018) 1220–1233.
[43] C. Li, L. Ma, Y. Liu, et al., TLR2 promotes development and progression of human glioma via enhancing autophagy, Gene 700 (2019) 52–59.
[44] C. Wang, et al., CD58 acts as a tumor promotor in hepatocellular carcinoma via activating the AKT/GSK-3β/β-catenin pathway, J. Transl. Med. 21 (1) (2023) 539, https://doi.org/10.1186/s12967-023-04364-4.
[45] Y. Li, et al., PAX5 epigenetically orchestrates CD58 transcription and modulates blinatumomab response in acute lymphoblastic leukemia, Sci. Adv. 8 (50) (2022) eadd6403, https://doi.org/10.1126/sciadv.add6403.
[46] P. Ho, et al., The CD58-CD2 axis is co-regulated with PD-L1 via CMTM6 and shapes anti-tumor immunity, Cancer Cell 41 (7) (2023) 1207–1221.e12, https://doi.org/10.1016/j.ccell.2023.05.014.
[47] B. Miao, et al., CMTM6 shapes antitumor T cell response through modulating protein expression of CD58 and PD-L1, Cancer Cell 41 (10) (2023) 1817–1828.e9, https://doi.org/10.1016/j.ccell.2023.08.008.